Unconventional isotope effects in the high-temperature cuprate superconductors

2001 J. Phys.: Condens. Matter 13 R569

(http://iopscience.iop.org/0953-8984/13/29/202)

INSTITUTE OF PHYSICS PUBLISHING JOURNAL OF PHYSICS: CONDENSED MATTER

J. Phys.: Condens. Matter **13** (2001) R569–R587 PII: S0953-8984(01)23775-8

REVIEW ARTICLE

Unconventional isotope effects in the high-temperature cuprate superconductors

Guo-meng Zhao[1,3], **H Keller**[1] **and K Conder**[2]

[1] Physik-Institut der Universität Zürich, CH-8057 Zürich, Switzerland
[2] Laboratory for Neutron Scattering, ETH Zürich and PSI Villigen, CH-5232 Villigen PSI, Switzerland

E-mail: gmzhao@uh.edu

Received 9 April 2001, in final form 29 May 2001
Published 6 July 2001
Online at stacks.iop.org/JPhysCM/13/R569

Abstract

We review various isotope effects in the high-T_c cuprate superconductors to assess the role of the electron–phonon interaction in the basic physics of these materials. Of particular interest are the unconventional isotope effects on the supercarrier mass, on the charge-stripe formation temperature, on the pseudogap formation temperature, on the electron paramagnetic resonance (EPR) linewidth, on the spin-glass freezing temperature and on the antiferromagnetic ordering temperature. The observed unconventional isotope effects strongly suggest that lattice vibrations play an important role in the microscopic pairing mechanism of high-temperature superconductivity.

1. Introduction

Developing a correct microscopic theory for high-T_c superconductivity is one of the most challenging problems in condensed matter physics. More than ten years after the discovery of the high-T_c cuprate superconductors by Bednorz and Müller [1], there have been no microscopic theories that can describe the physics of high-T_c superconductors completely and unambiguously. Due to the high T_c values and the earlier observation of a small oxygen-isotope effect in a 90 K cuprate superconductor $YBa_2Cu_3O_{7-y}$ [2–4], many theorists believe that the electron–phonon interaction cannot be the origin of high-T_c superconductivity. Most physicists have thus turned their minds towards an alternative pairing interaction of purely electronic origin (e.g., see [5–7]). As a matter of fact, the idea that the highest T_c is only 30 K within the conventional phonon-mediated mechanism is not justified. In principle, T_c can increase monotonically with both the phonon frequency and the electron–phonon coupling constant within the phonon-mediated Eliashberg theory [8]. The limitation of the T_c within

[3] Present address: Department of Physics and Texas Center for Superconductivity, University of Houston, Houston, Texas 77204, USA

the phonon mechanism is only imposed by a possible structural instability in the case of too strong an electron–phonon interaction. However, there is no universally accepted, simple, and quantitative stability criterion [8].

It is well known that the observation of a gap in the electronic excitation spectrum [9] and the discovery of an isotope effect [10, 11] in conventional superconductors provided important and crucial clues to the understanding of the microscopic mechanism of superconductivity. In particular, the effect of changing isotope mass on the superconducting transition temperature T_c implies that superconductivity is not of purely electronic origin, but that lattice vibrations (phonons) play an important role in the microscopic mechanism for this phenomenon.

The first piece of evidence for an isotope effect was reported in 1950 by Maxwell [10] and, independently, by Reynolds *et al* [11]. They found that the critical temperature T_c of mercury is an inverse function of the isotope mass. In the same year Fröhlich [12] pointed out that the same electron–lattice interaction which describes the scattering of conduction electrons by lattice vibrations gives rise to an indirect interaction between electrons. He proposed that this indirect interaction is responsible for superconductivity. Fröhlich's theory got strong support from the observed isotope effect, and played a decisive role in establishing a correct mechanism. In 1956, Cooper [13] demonstrated that electrons with an attractive interaction form bound pairs (so-called Cooper pairs) which lead to superconductivity. However, the existence of electron pairs does not necessarily imply a phonon-mediated pairing. Indeed, Bose condensation, as considered in 1955 by Schafroth [14], is also a possible mechanism for superconductivity, but the model was not able to explain the isotope effect. Finally, in 1957, Bardeen, Cooper and Schrieffer (BCS) [15] developed their theory which can explain most physical properties observed in conventional superconductors.

Remarkably, the BCS theory can well explain the isotope effect. The T_c within the theory is given by

$$k_B T_c = 1.13\hbar\omega_D \exp\left(-\frac{1}{N(0)V}\right) \tag{1}$$

where ω_D is the Debye frequency, which is proportional to $M^{-1/2}$. The electron–phonon coupling $N(0)V$ is the product of the electron–phonon interaction strength V and the electronic density of states at the Fermi surface $N(0)$, both of which are independent of the ion mass M in the harmonic approximation. Equation (1) implies an isotope–mass dependence of T_c, with an isotope-effect exponent $\alpha = -\mathrm{d}\ln T_c/\mathrm{d}\ln M = 1/2$. This is in excellent agreement with the reported isotope effects in the non-transition metal superconductors (e.g., Hg, Sn and Pb). In fact, the isotope effect was the first justification of the proposed electron–phonon coupling mechanism.

The conventional phonon-mediated superconducting theory is based on the Migdal adiabatic approximation in which the phonon-induced electron self-energy is given correctly to the order of $(m_b/M)^{1/2} \sim 10^{-2}$, where m_b is the bare mass of an electron. Within this approximation, the density of states at the Fermi level $N(0)$, the electron–phonon coupling constant λ_{ep} and the effective mass of the supercarriers are all independent of the ion mass M. However, if the interactions between electrons and nuclear ions are strong enough for electrons to form polarons (quasiparticles dressed by lattice distortions), their effective mass m^* will depend on M. This is because the polaron mass $m^* = m_b \exp(A/\omega)$ [16], where A is a constant and ω is a characteristic optical phonon frequency which depends on the masses of ions. Hence there is a large isotope effect on the carrier mass in polaronic metals, in contrast to the zero isotope effect in ordinary metals. The total exponent of the isotope effect on m^* is defined as $\beta = \sum -\mathrm{d}\ln m^*/\mathrm{d}\ln M_i$ (M_i is the mass of the ith atom in a unit cell). From this

definition and the expression for the polaron mass m^* mentioned above, one readily finds

$$\beta = -\tfrac{1}{2}\ln(m^*/m_b). \tag{2}$$

The above equation implies that there should be a large negative isotope effect on m^* in polaronic metals.

Therefore, if the electron–phonon interaction is strong enough to form polarons and/or bipolarons, one will expect a substantial isotope effect on the effective mass of carriers. In this article, we will present various isotope effects in cuprates, including unconventional isotope effects on the supercarrier mass, on the charge-stripe formation temperature, on the pseudogap formation temperature, on the EPR linewidth, on the spin-glass freezing temperature and on the antiferromagnetic ordering temperature. These unconventional isotope effects clearly demonstrate that phonons are relevant to the basic physics of cuprates and may be important for the occurrence of high-temperature superconductivity.

2. Isotope effect on the superconducting transition temperature

Studies of isotope shifts of T_c have been carried out in almost all known cuprates. A comprehensive review was given by Franck [17]. The role of the anharmonicity of the apical oxygen on the isotope effect was discussed in detail by Müller [18]. Most of the studies reported so far concern the oxygen-isotope shift (OIS) of T_c by replacing ^{16}O with ^{18}O, partly because the experimental procedures are simple and reliable. Now it is generally accepted that optimally-doped cuprates exhibit a small and positive oxygen-isotope exponent α_O. It was also found that α_O for optimally-doped materials decreases with increasing T_c [19]. The small OIS observed in the optimally doped cuprates suggest that phonons might not be important in bringing about high-temperature superconductivity.

However, the doping dependence of the OIS has been extensively studied in different cuprate systems [17, 20–27]. For a particular family of doped cuprates the OIS increases with decreasing T_c, and can be even larger than the BCS value. In figure 1(a) we plot the doping dependence of T_c for the ^{16}O and ^{18}O samples of the single-layer cuprate $La_{2-x}Sr_xCuO_4$. It is clear that the T_c's of the ^{18}O samples are always lower than those of the ^{16}O samples. The doping dependence of the isotope exponent α_O is shown in figure 1(b). The magnitude of α_O increases with a decrease of doping and becomes very large (>0.5) in the deeply underdoped regime. The large α_O value observed near $x = 0.125$ might be related to a structural instability [28]. The results suggest that the phonon modes related to the oxygen vibrations are strongly coupled to conduction electrons.

In addition to the large OISs observed in underdoped compounds, there are also large copper isotope shifts observed in underdoped $La_{2-x}Sr_xCuO_4$ [22], oxygen-depleted $YBa_2Cu_3O_{7-y}$ [29], Pr-substituted $Y_{1-x}Pr_xBa_2Cu_3O_{7-y}$ [30] and $Y_{1-x}Pr_xBa_2Cu_4O_8$ [30], as well as in $YBa_2Cu_4O_8$ [31]. In figure 2, we plot the oxygen and copper isotope exponents as functions of T_c in $Y_{1-x}Pr_xBa_2Cu_3O_{7-y}$ and $Y_{1-x}Pr_xBa_2Cu_4O_8$. As T_c or doping decreases, both α_O and α_{Cu} increase monotonously. Interestingly, α_{Cu} is about three-quarters of α_O in the deeply underdoped region, while α_{Cu} is even larger than α_O near the optimal doping. This suggests that the Cu-dominated phonon modes (most of them are low-energy modes) are involved in the superconducting pairing.

The large copper-isotope shift also implies that the phonons in the CuO_2 planes are relevant to superconductivity. By analogy, one should also expect that the planar oxygen vibrations make more important contributions to the pairing than the apical and/or chain oxygen vibrations. We can distinguish the contributions of the different oxygen sites to the total OIS by site-selective oxygen-isotope experiments. A partially site-selective oxygen-isotope exchange

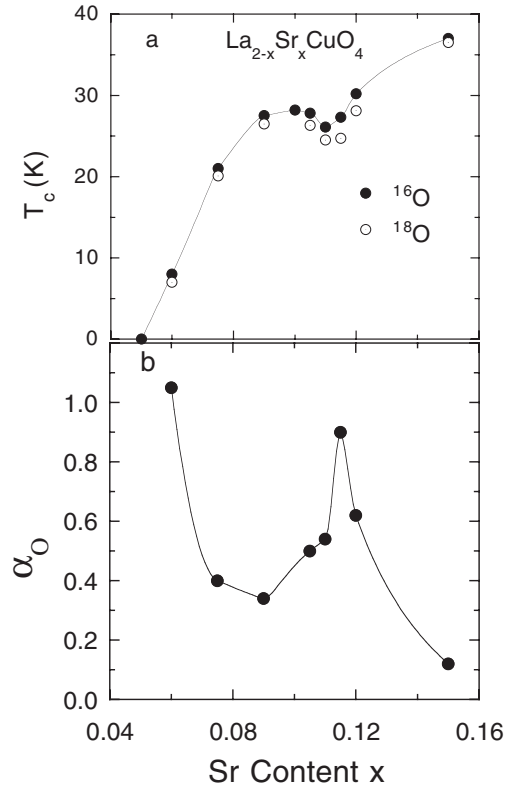

Figure 1. Dependences of (a) T_c and (b) the oxygen-isotope exponent α_O on the Sr content x for ^{16}O and ^{18}O samples in $La_{2-x}Sr_xCuO_4$. After [27].

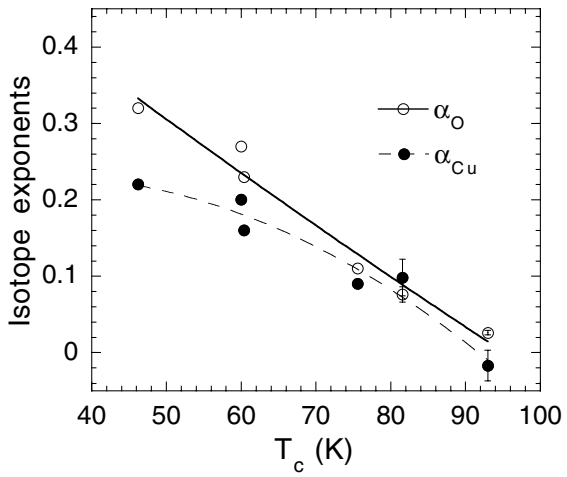

Figure 2. The oxygen and copper isotope exponents as a function of T_c for $Y_{1-x}Pr_xBa_2Cu_3O_{7-y}$ and $Y_{1-x}Pr_xBa_2Cu_4O_8$. The data were taken from [29–31].

was attempted by Cardona *et al* [32] and by Ham *et al* [33]. The experimental difficulty in doing a complete site-selective oxygen-isotope exchange was overcome by Nickel *et al* [34]. In their experiment the authors replaced the ^{18}O by ^{16}O in the chain and apical oxygen sites of a fully ^{18}O exchanged $YBa_2Cu_3O_7$ sample, while keeping the ^{18}O unexchanged in the plane sites. The site-selectivity was confirmed by Raman spectroscopy [34]. A small negative OIS ($\alpha_O = -0.010(4)$) associated with the planar oxygen was found. In contrast, Zech *et al* [35]

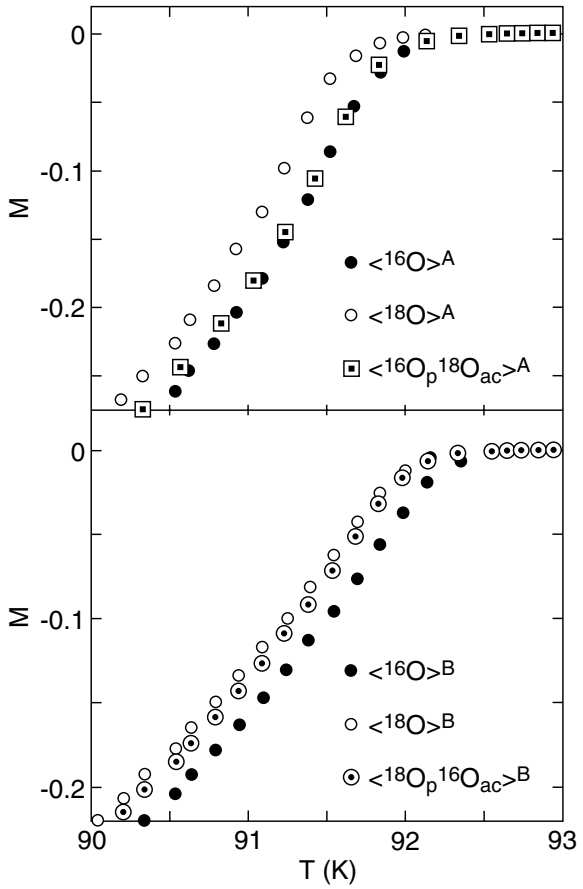

Figure 3. The site-selective oxygen-isotope effect in $YBa_2Cu_3O_{6.96}$. Here $\langle {}^{18}O_p\ {}^{18}O_{ac}\rangle$ means all the oxygen sites are exchanged by ^{18}O, and $\langle {}^{18}O_p\ {}^{16}O_{ac}\rangle$ means that only the in-plane oxygen sites are replaced by ^{18}O. It is evident that the planar oxygen mainly (>80%) contributes to the total OIS in the optimally doped cuprate. After [35].

showed a small positive OIS ($\alpha_O = 0.018(4)$) related to the planar oxygen ions. The above discrepancy may be due to a broad superconducting transition in the samples of Nickel *et al* [34], which makes it difficult to define T_c reliably. Although the OIS is small in the optimally-doped samples, the experiment carried out by Zech *et al* [35] provided evidence that the planar oxygen ions mainly (80%) contribute to the total OIS (see figure 3). Nevertheless it is not obvious that the same conclusion should apply to the underdoped samples where the total OIS is large. Zhao *et al* [36] thus carried out site-selective oxygen-isotope experiments in underdoped and optimally doped samples of $Y_{1-x}Pr_xBa_2Cu_3O_{7-y}$. In figure 4, we show the results of the site-selective oxygen-isotope effect for optimally doped $YBa_2Cu_3O_{6.94}$. It is striking that the results shown in figure 4 are in excellent agreement with those in figure 3. This indicates the good reproducibility of these experiments. The results for underdoped $Y_{0.7}Pr_{0.3}Ba_2Cu_3O_{6.97}$ are plotted in figure 5. Remarkably, the planar oxygen ions mainly (>80%) contribute to the total OIS in the underdoped samples as well. In figure 6, we show the total isotope shift as a function of T_c for $Y_{1-x}Pr_xBa_2Cu_3O_{7-y}$ together with the isotope shifts from the planar oxygen ions as well as from the apical and chain oxygen ions. From this figure, one can clearly see that the planar oxygen ions make a predominant contribution to the total OIS in all the doping levels.

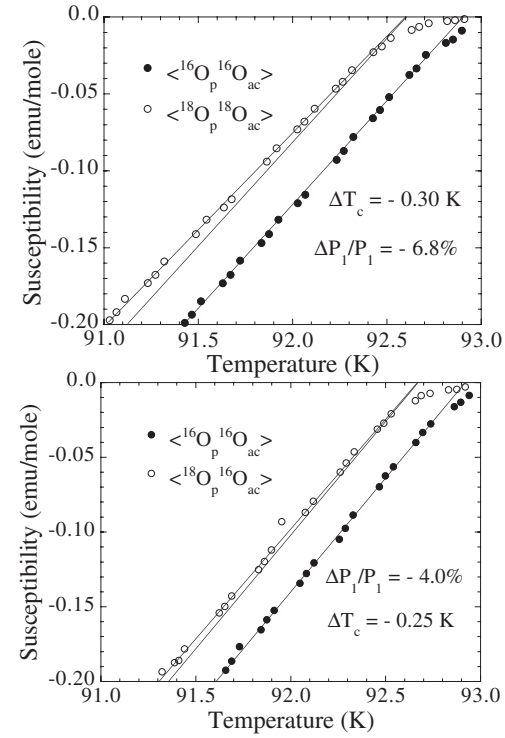

Figure 4. The site-selective oxygen-isotope effect in an optimally doped $YBa_2Cu_3O_{6.94}$. After [36].

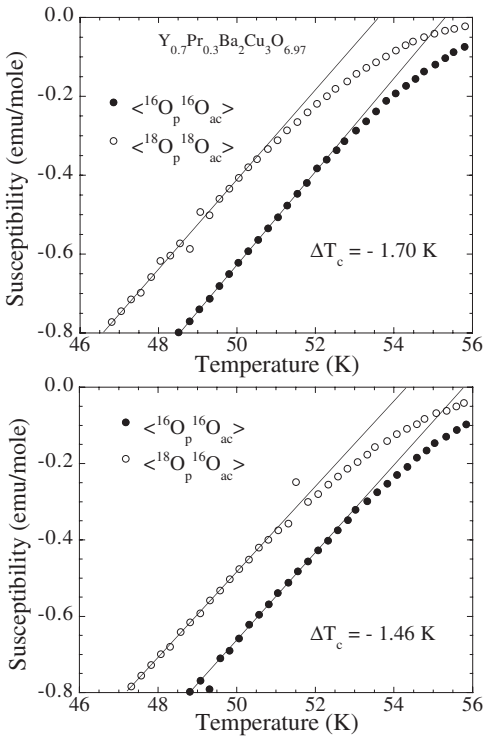

Figure 5. The site-selective oxygen-isotope effect in an underdoped $Y_{0.7}Pr_{0.3}Ba_2Cu_3O_{6.97}$. The results show that the planar oxygen mainly (>80%) contributes to the total OIS in this underdoped cuprate. After [36].

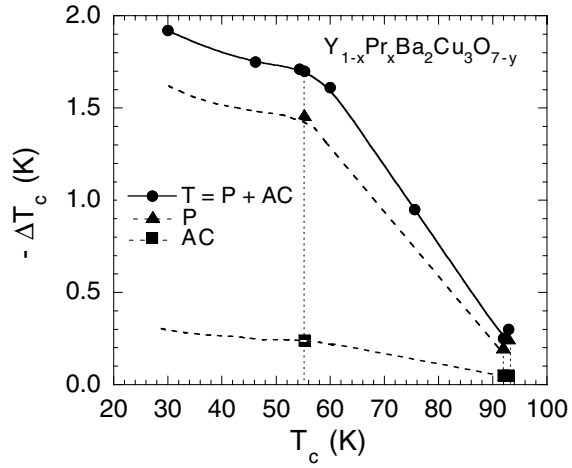

Figure 6. The total (T) isotope shifts as a function of T_c for $Y_{1-x}Pr_xBa_2Cu_3O_{7-y}$ together with the isotope shifts from the planar (P) oxygen ions as well as from the apical and chain (AC) oxygen ions. The partial data of the total OISs are taken from [17] and have been corrected for 100% oxygen-isotope exchange. The other data are from [35, 36].

3. Negligible oxygen-isotope effect on the carrier density

From the above results, an important question arises: are the observed large isotope shifts in underdoped cuprates caused by a possible difference in the carrier densities of two isotope samples or by a strong electron–phonon coupling? It is very unlikely that the isotope effect is due to a difference in the carrier densities of two isotope samples. This is because the T_c's of the ^{18}O samples are always lower than the ^{16}O samples by more than 1 K in the underdoped region, independent of whether dT_c/dx is positive, negative or zero (see figure 1(a)).

There are three indirect experiments which have demonstrated that the difference in the hole densities of the ^{16}O and ^{18}O samples is less than 0.0002 per Cu site [25–27]. Now we are able to determine the oxygen content very accurately using very precise volumetric analysis [37]. Figure 7 shows the oxygen content of the ^{16}O and ^{18}O samples of $La_{2-x}Sr_xCuO_4$ with different doping x. It is remarkable that the oxygen content of the two isotope samples are the same within ± 0.0002 per Cu site. These experiments consistently show that the difference in the hole densities of the ^{16}O and ^{18}O samples is negligible, so that the observed large isotope effects are intrinsic and caused by a strong electron–phonon interaction.

4. Large oxygen-isotope effect on the effective supercarrier mass

Several groups [21, 22] noticed that there is an isotope effect on the diamagnetic Meissner signal in decoupled fine-grained samples. Zhao *et al* [25] carefully studied this effect and interpreted it as due to the isotope–mass dependence of the average supercarrier mass m^{**} ($\equiv\sqrt[3]{(m_{ab}^{**})^2 m_c^{**}}$). Since the magnetic penetration depth $\lambda(0)$ is proportional to $\sqrt{m^{**}/n_s}$, then

$$\Delta m^{**}/m^{**} = 2\Delta\lambda(0)/\lambda(0) + \Delta n_s/n_s \tag{3}$$

where Δ means any small change of a quantity upon isotope substitution. Thus the isotope dependence of m^{**} can be determined if one can independently measure the isotope dependence of $\lambda(0)$ and of n_s. As shown above, there is a negligible oxygen-isotope effect on the normal carrier density n, and $n_s = n$ for clean superconductors, so one should expect no significant

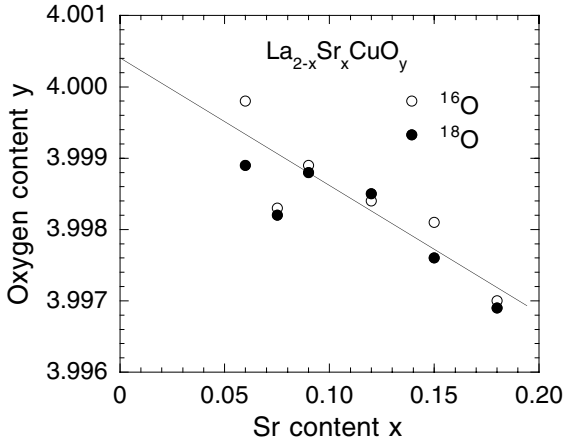

Figure 7. The oxygen contents of the ^{16}O and ^{18}O samples of $La_{2-x}Sr_xCuO_y$ with different doping x (unpublished data). The oxygen content was determined from a very precise volumetric analysis [37]. The weight of each sample used for the analysis is about 500 mg. The oxygen content can be determined more precisely for a higher x and a heavier sample. The oxygen content of two isotope samples are the same within ± 0.0002 per Cu site.

isotope effect on n_s. Indeed, there is a negligible oxygen-isotope effect on the supercarrier density n_s in $YBa_2Cu_3O_{6.94}$ [38].

The isotope dependence of $\lambda(0)$ can be determined from that of the Meissner fraction $f(0)$ which, for decoupled and fine-grained samples, depends on the penetration depth $\lambda(0)$ and on the average grain radius R, as seen from the Shoenberg formula for spherical grains [39]:

$$f(T) = \frac{3}{2}\left[1 - 3\left(\frac{\lambda(T)}{R}\right)\coth\left(\frac{R}{\lambda(T)}\right) + 3\left(\frac{\lambda(T)}{R}\right)^2\right] \tag{4}$$

where $\lambda(T) = \sqrt[3]{[(\lambda_{ab}(T)]^2\lambda_c(T)}$ for layered compounds [40]. From equation (4) it is obvious that a change in $\lambda(0)$ will lead to a change in $f(0)$, which implies that the isotope dependence of $\lambda(0)$ can be determined from the isotope dependence of $f(0)$.

In figure 8, we show the Meissner effects for the ^{16}O and ^{18}O samples of $La_{2-x}Sr_xCuO_4$ with $x = 0.06$ and 0.105. The samples are loosely packed with rather small grain sizes ($R \approx 2$–4 μm). One can clearly see that there are large oxygen isotope effects on both T_c and the Meissner fraction. The most remarkable result is that the Meissner fraction of the ^{18}O sample is lower than that for the ^{16}O sample by about 23% in the case of $x = 0.06$. The isotope effects are reversible upon the isotope back-exchange [26, 27], and reproducible in several sets of samples. For $x = 0.06$, we evaluate $\Delta m^{**}/m^{**} = 24(2)\%$. This indicates a large negative oxygen-isotope effect on the effective supercarrier mass in the deeply underdoped cuprates.

The above results were obtained from powder samples and correspondingly reflect the average properties of those highly anisotropic superconductors. To gain more insight, it is essential to determine the oxygen-isotope effect on the inplane effective supercarrier mass m_{ab}^{**}. Although we have tentatively extracted the isotope dependence of m_{ab}^{**} from experiments on powder samples [26], more reliable results should be obtained from experiments on single crystals.

Unfortunately, complete oxygen-isotope exchange by gas diffusion is impossible in single crystals of large volume. In order to reach complete oxygen-isotope exchange, microcrystals with a volume of $V \approx 150 \times 150 \times 50$ μm^3 (mass ≈ 10 μg) should be

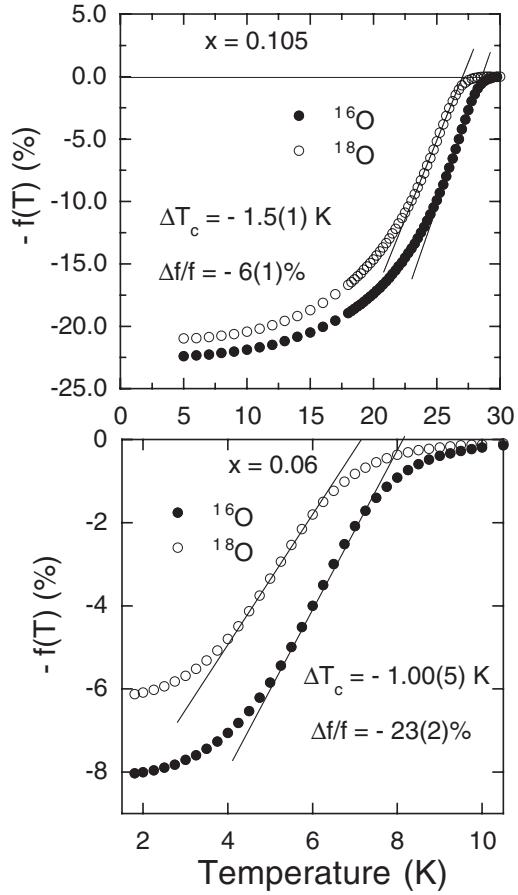

Figure 8. The Meissner fractions for the ^{16}O and ^{18}O samples of $La_{2-x}Sr_xCuO_4$ with $x = 0.06$ and 0.105. After [26, 27].

used. In this case, commercial SQUID magnetometers do not have enough sensitivity to measure the magnetization for such tiny crystals, especially near T_c. Fortunately our highly sensitive torque magnetometer [41] is able to detect the small diamagnetic signal for the tiny crystals.

The superconducting transition was studied by cooling the sample in a magnetic field $B_a = 0.1$ T applied at an angle of 45° with respect to the c-axis [42]. The torque signal was continuously recorded upon cooling the sample at a cooling rate of 0.01 K s^{-1}. In order to determine the background signal of the cantilever, the measurement was repeated in zero field and the data were subtracted from those of the field cooled measurement. The magnetic torque against temperature data obtained for crystals with $x = 0.086$ and 0.080 are shown in figure 9. It is clear that T_c is lower for the ^{18}O exchanged samples. Furthermore, the magnetic signals of the back-exchanged samples (cross symbols) coincide with those of the ^{16}O annealed samples (open circles). We define T_c as the temperature where the linearly extrapolated transition slope intersects the base line. The relative changes in T_c are found to be $\Delta T_c/T_c = -5.5(4)\%$ for $x = 0.080$ and $-5.1(3)\%$ for $x = 0.086$. The exponent α_O is found to be 0.47(2) for $x = 0.080$ and 0.40(2) for $x = 0.086$, which is in good agreement with the results obtained

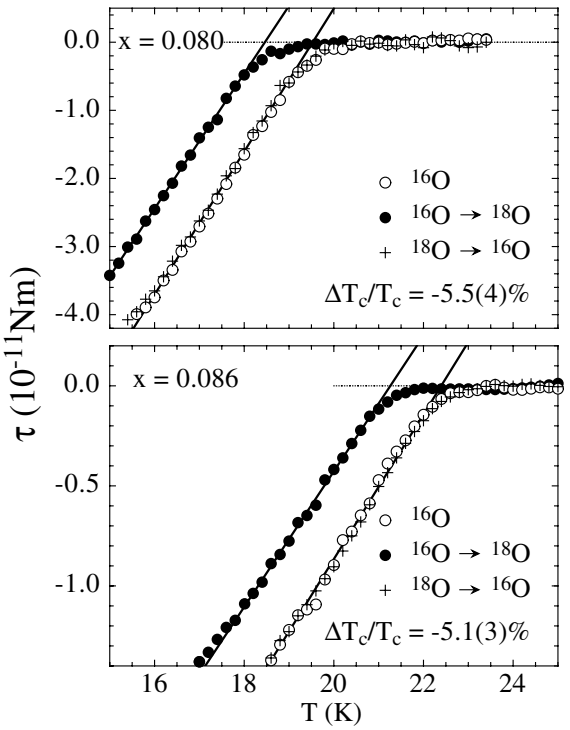

Figure 9. The magnetic torque as a function of temperature for the ^{16}O and ^{18}O microcrystals of $La_{2-x}Sr_xCuO_4$ with $x = 0.086$ and 0.080. The measurements were carried out in a magnetic field $B_a = 0.1$ T applied at an angle of 45° with respect to the c-axis. After [42].

for powder samples with similar doping levels [20, 27].

More interestingly, the in-plane penetration depth $\lambda_{ab}(T)$ can be extracted from field-dependent measurements [42]. Figure 10 displays $\lambda_{ab}^{-2}(T)$ for the isotope-exchanged crystals with $x = 0.086$ and 0.080. The temperature dependence is described by the power law $\lambda_{ab}^{-2}(T) = \lambda_{ab}^{-2}(0)[1 - (T/T_c)^n]$ with an exponent $n \approx 5$. From figure 10 it is evident that both T_c and $\lambda_{ab}^{-2}(0)$ shift down upon replacing ^{16}O by ^{18}O. The shifts are found to be $\Delta\lambda_{ab}^{-2}(0)/\lambda_{ab}^{-2}(0) = -9(3)\%$ and $-7(1)\%$ for $x = 0.080$ and 0.086, respectively. Using $\Delta n_s = 0$, we find $\Delta m_{ab}^{**}/m_{ab}^{**} = 9(3)\%$ for $x = 0.080$, and 7(1)% for $x = 0.086$.

Moreover, a substantial value of $\Delta m_{ab}^{**}/m_{ab}^{**} = 5$–$6\%$ was also obtained for several optimally doped cuprates (e.g. $YBa_2Cu_3O_{6.94}$, $La_{1.85}Sr_{0.15}CuO_4$ and $Bi_{1.6}Pb_{0.4}Sr_2Ca_2Cu_3O_{10+y}$) from magnetization measurements [43]. Very recent muon-spin rotation experiments on the oxygen-isotope exchanged $YBa_2Cu_3O_{6.96}$ have confirmed that $\Delta m_{ab}^{**}/m_{ab}^{**} \simeq 5\%$. Therefore, there is a substantial isotope effect on the in-plane supercarrier mass in optimally doped cuprates, but a very small effect on T_c. Such unusual isotope effects place strong constraints on the pairing mechanism of high-temperature superconductivity.

5. Huge oxygen-isotope effect on the charge-stripe formation temperature

One of the most remarkable findings in the high-temperature copper oxide superconductors is the formation of alternating spin and charge stripes below a characteristic temperature [44, 45]. Various x-ray absorption spectroscopic measurements [46] suggest that the local structures in

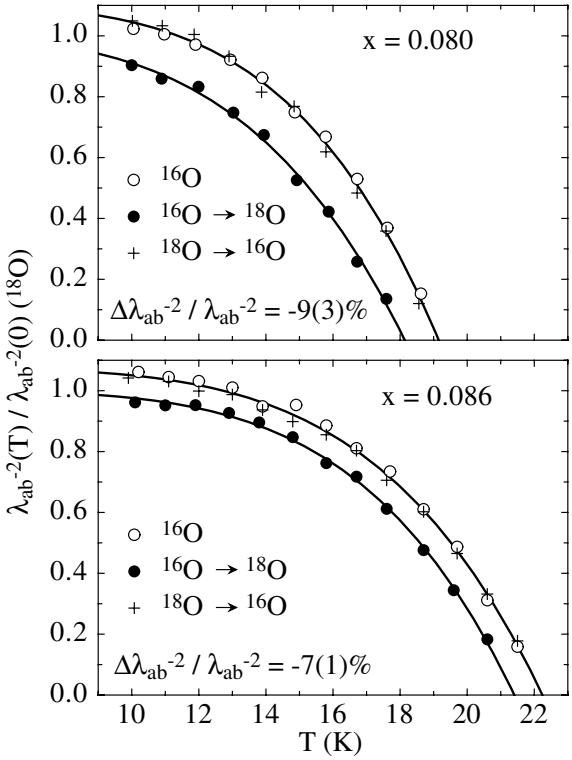

Figure 10. The in-plane penetration depth $\lambda_{ab}^{-2}(T)$ for the ^{16}O and ^{18}O microcrystals of $La_{2-x}Sr_xCuO_4$ with $x = 0.086$ and 0.080. The $\lambda_{ab}^{-2}(T)$ value was extracted from the field dependence of the torque. After [42].

the alternating stripes are different, forming an incommensurate superlattice. Such a stripe phase is believed to be important to the understanding of the pairing mechanism of high-temperature superconductivity [47]. However, the microscopic origin of the stripe phase is still highly debated. It could be caused by purely electronic interactions [47] and/or by a strong electron–phonon interaction [48].

Although there is increasing experimental evidence for a strong electron–phonon interaction in the cuprate superconductors, it is not clear whether this interaction is important to the formation of the stripe phase. For the colossal magnetoresistive manganites, a strong electron–phonon interaction plays an essential role in the formation of the Jahn–Teller stripes (or charge ordering), as inferred from a very large OIS of the charge-ordering temperature observed in both $Nd_{0.5}Sr_{0.5}MnO_3$ and $La_{0.5}Ca_{0.5}MnO_3$ systems [49]. Therefore it seems natural to seek an isotope effect on the stripe formation temperature in cuprates.

X-ray absorption near edge spectroscopy (XANES) is a powerful technique to probe the local structure conformations for a system. From the XANES data, two characteristic peaks denoted by A and B in the XANES spectra of the cuprates are identified, which characterize the local structures within and out of the CuO_2 planes. A parameter R is defined as $R = (\beta_1 - \alpha_1)/(\beta_1 + \alpha_1)$, where β_1 and α_1 are the intensities of peak A and peak B in the XANES spectra, respectively. When charge-stripe ordering occurs, a change in the local structure takes place, leading to a sudden increase in R below the charge-stripe formation temperature T^*. The identification of T^* by XANES has been tested in a compound $La_{1.875}Ba_{0.125}CuO_4$ where T^*

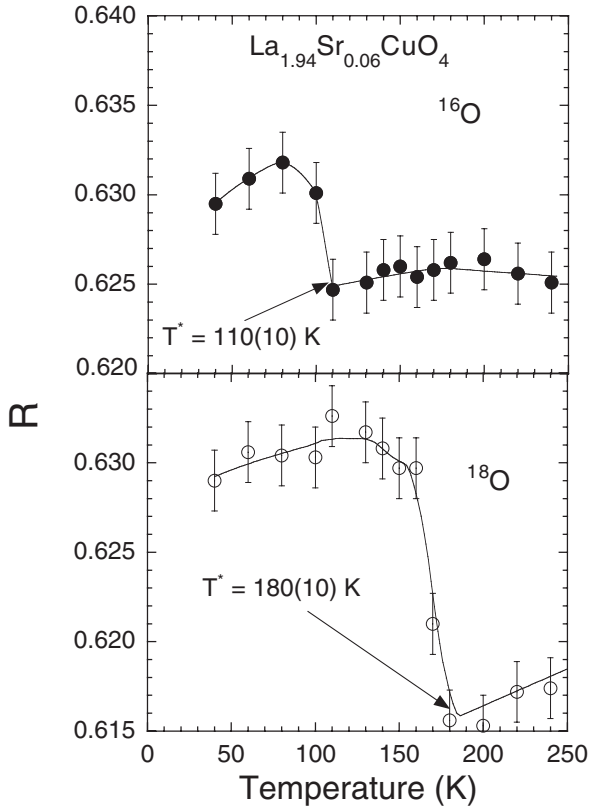

Figure 11. The temperature dependence of the parameter R for the oxygen-isotope exchanged $La_{1.94}Sr_{0.06}CuO_4$. See text for the definition of the parameter R. After [50].

was determined by other techniques [50]. In figure 11, we show the temperature dependence of the parameter R for the oxygen isotope exchanged $La_{1.94}Sr_{0.06}CuO_4$. From the figure, one can clearly see that, upon replacing ^{16}O with ^{18}O, the charge-stripe formation temperature T^* in this cuprate increases from about 110 K to 180 K. Such a large negative isotope effect on charge ordering can be explained in terms of electron–phonon coupling beyond the Migdal approximation [51].

6. Oxygen-isotope effects on the pseudogap formation temperature

Recently, a neutron spectroscopic investigation of the isotope effect on the relaxation rate of crystal field excitations of Ho^{3+} in $HoBa_2Cu_4O_8$ was carried out [52]. In figure 12, we plot the temperature dependence of the intrinsic linewidth $\Gamma(T)$ (corresponding to the $\Gamma_3^{(1)} \rightarrow \Gamma_4^{(1)}$ transition of Ho^{3+}) for the ^{16}O and ^{18}O samples. In the high-temperature range, the linewidth appears to exhibit a linear temperature dependence. Cooling down to a characteristic temperature T^p, the linewidth suddenly gets narrower. Of particular interest is the characteristic temperature T^p which strongly depends on the oxygen-isotope mass. Upon replacing ^{16}O by ^{18}O, T^p changes from 170 K to 220 K, i.e. there is a large oxygen-isotope effect on T^p ($\approx$50 K). Similarly, a large copper-isotope effect on T^p has been found in the same compound [53]. The huge oxygen-isotope effects on T^* [50] and on T^p [52] indicate

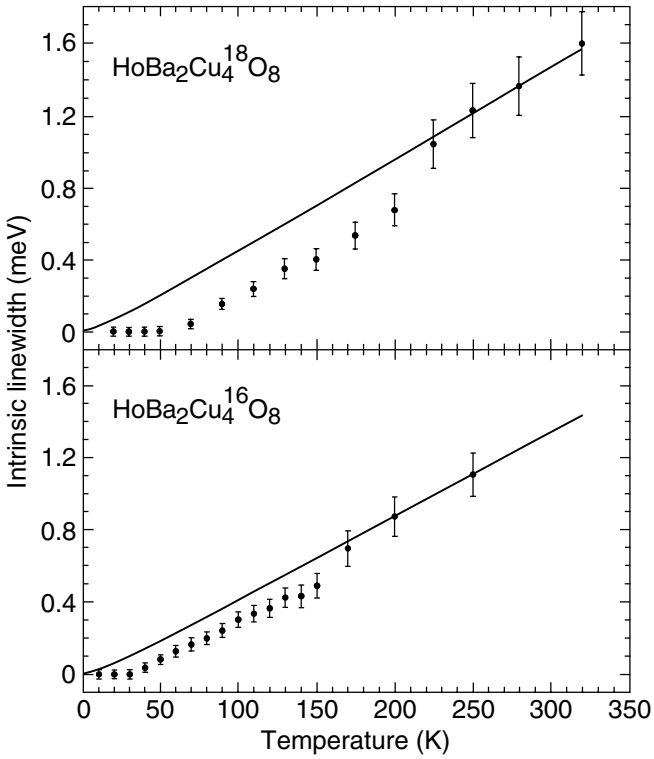

Figure 12. Temperature dependence of the intrinsic linewidth $\Gamma(T)$ of the $\Gamma_3^{(1)} \rightarrow \Gamma_4^{(1)}$ transition of Ho^{3+} for the ^{16}O and ^{18}O samples of $HoBa_2Cu_4O_8$. After [52].

that a strong electron–phonon interaction plays an essential role in the charge dynamics and superconductivity [48]. Although the authors of [52] attributed the characteristic temperature T^p to a pseudogap formation temperature, one cannot rule out the possibility that T^p may be related to dynamical charge ordering. We would like to mention that a small positive oxygen-isotope effect on the spin pseudogap has been observed in $YBa_2Cu_4O_8$ [54].

7. Oxygen-isotope effect on the electron paramagnetic resonance linewidth

Electron paramagnetic resonance (EPR) is a powerful technique to probe and understand various phenomena in solid-state physics. Unfortunately, the intrinsic Cu^{2+} signals in the cuprate superconductors have not been observed except for those of chain fragments in $YBa_2Cu_3O_{6+\delta}$ ($0.7 < \delta < 0.9$) [55] and three-spin polarons [56]. The EPR silence has been attributed by many researchers to the very fast relaxation time of the Cu^{2+} spins. In order to test this possibility, one needs to dope the material with a paramagnetic S-state ion (e.g. Mn^{2+}). Its relaxation occurs via the fast relaxing carriers. This is called bottleneck effect, which has indeed been observed in Mn^{2+} doped $La_{2-x}Sr_xCuO_4$ [57].

Here we focus on the oxygen-isotope effect on the EPR linewidth in the Mn^{2+} doped $La_{2-x}Sr_xCuO_4$ [58, 59]. In figure 13, we show the temperature dependence of the EPR linewidth ΔH_{pp} for ^{16}O isotope samples of $La_{2-x}Sr_xCu_{0.98}Mn_{0.02}O_4$ with $x = 0.03$, 0.06, and 0.10 (figure 13(a)), as well as the isotope effect on the EPR linewidth ΔH_{pp} in

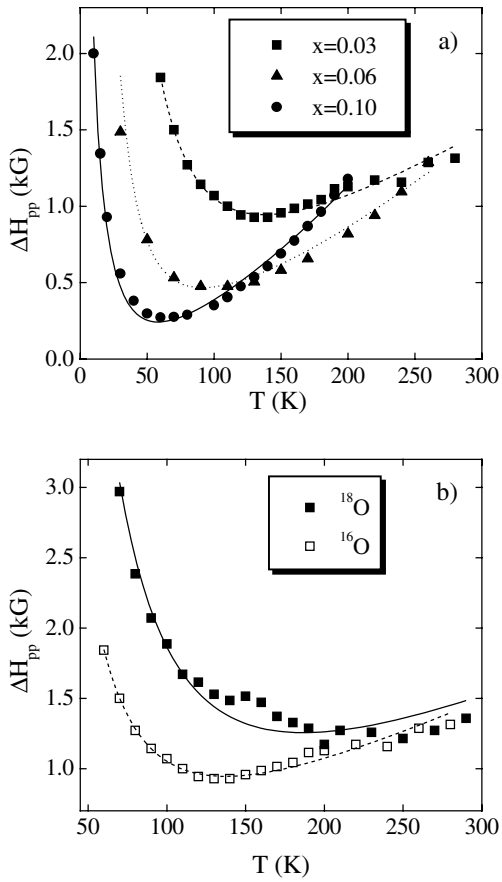

Figure 13. (a) Temperature dependence of the EPR linewidth ΔH_{pp} for ^{16}O isotope samples of $La_{2-x}Sr_xCu_{0.98}Mn_{0.02}O_4$ with $x = 0.03, 0.06$ and 0.10. (b) The oxygen-isotope effect on the EPR linewidth ΔH_{pp} in $La_{1.97}Sr_{0.03}Cu_{0.98}Mn_{0.02}O_4$. After [58, 59].

$La_{1.97}Sr_{0.03}Cu_{0.98}Mn_{0.02}O_4$ (figure 13(b)). It is remarkable that the EPR linewidth at 100 K for the ^{16}O sample is about half the one for the ^{18}O sample. Such a large oxygen-isotope effect on the linewidth indicates that the dynamics of the oxygen atoms play a key role in the Cu^{2+} relaxation. Interestingly, the temperature dependences of the linewidth for both isotope samples are in good agreement with theoretical calculations (see solid and dashed lines) [58, 59].

8. Large oxygen-isotope effect on the spin-glass freezing temperature

The parent compounds of the cuprate superconductors exhibit long-range three-dimensional (3D) antiferromagnetic (AF) order, which is rapidly destroyed as holes are doped into the CuO_2 planes. A short-range-ordered AF state exists at doping of $0.02 < x < 0.06$ in $La_{2-x}Sr_xCuO_4$. Early muon spin rotation (μSR) and neutron scattering experiments found that this magnetic state resembles a spin glass [60]. More detailed studies using ^{139}La nuclear quadrupole resonance [61] showed that the magnetic state in this doping regime is not a conventional

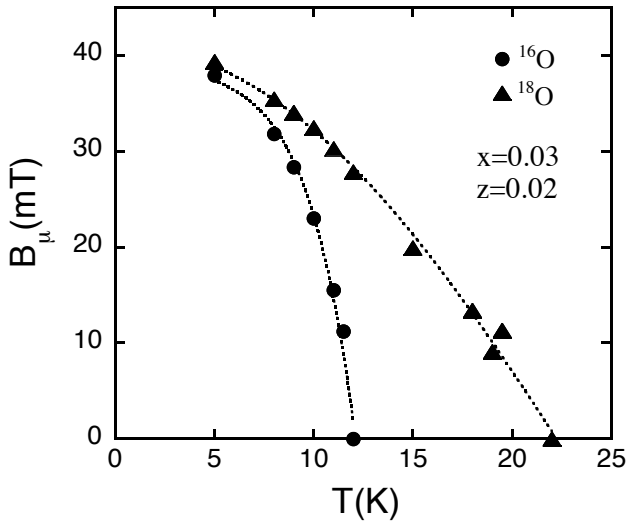

Figure 14. Temperature dependence of the internal magnetic fields B_μ (probed by μSR) for the ^{16}O and ^{18}O samples of $La_{1.97}Sr_{0.03}Cu_{0.98}Mn_{0.02}O_4$. After [63].

spin glass, but a cluster spin glass (CSG). The understanding of how the short-range-ordered AF state affects superconductivity and how it is influenced by lattice vibrations will help to clarify the pairing mechanism of high-T_c superconductivity.

It is well known that conventional theories of magnetism neglect atomic vibrations; the atoms are mostly considered as being infinitely heavy in theoretical descriptions of magnetic phenomena, which rules out the existence of an isotope effect on magnetism. However, there is an exceptional example. In ferromagnetic manganites, a giant oxygen-isotope effect on the Curie temperature has been observed [62]. The question is whether such an isotope effect also exists in cuprates.

In figure 14, we show the temperature dependence of the internal magnetic fields B_μ (probed by μSR) for the ^{16}O and ^{18}O samples of $La_{1.97}Sr_{0.03}Cu_{0.98}Mn_{0.02}O_4$. It is remarkable that the spin-glass freezing temperature T_g almost doubles upon replacing ^{16}O by ^{18}O. Such a huge isotope effect on the spin-glass freezing temperature suggests that spin dynamics in cuprates is ultimately correlated with lattice vibrations.

9. Oxygen-isotope effect on the AF ordering temperature

The AF order observed in the parent insulating compounds like La_2CuO_4 signals a strong electron–electron Coulomb correlation. On the other hand, the large isotope effects found in the underdoped cuprate superconductors indicate a strong electron–phonon interaction. Now a question arises: can the strong electron–phonon interaction modify the AF exchange energy and thus the AF ordering temperature in the parent insulating compounds? Studies of the isotope effect on the AF ordering temperature could clarify this issue [64, 65].

Figure 15 shows the temperature dependence of the susceptibility for the ^{16}O and ^{18}O samples of undoped La_2CuO_4 (figure 15(a)) and of oxygen doped La_2CuO_{4+y} (figure 15(b)). One can see that the AF ordering temperature T_N for the ^{18}O sample is lower than the ^{16}O sample by about 1.9 K in the case of the undoped samples. For the oxygen-doped samples, there is a negligible isotope effect.

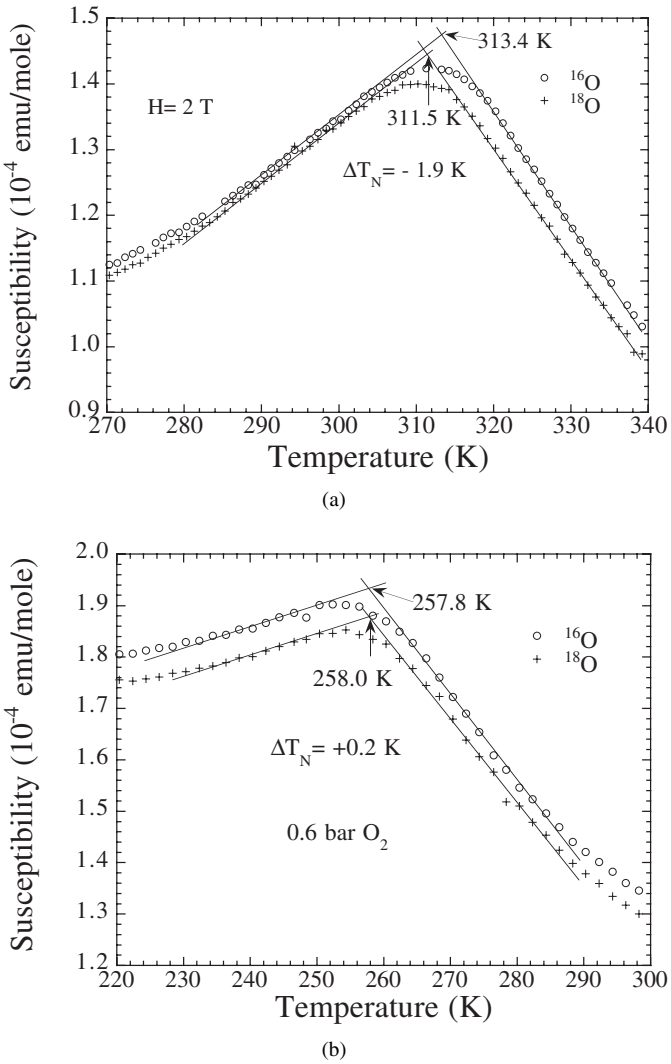

Figure 15. The temperature dependence of the susceptibility for the ^{16}O and ^{18}O samples of (a) undoped La_2CuO_4, and (b) oxygen-doped La_2CuO_{4+y}. After [64].

It is known that the AF properties of La_2CuO_{4+y} can be well understood within mean-field theory which leads to a T_N formula [66]:

$$k_B T_N = J'[\xi(T_N)/a]^2 \tag{5}$$

where J' is the interlayer coupling energy, $\xi(T_N)$ is the in-plane AF correlation length at T_N with $\xi(T_N) \propto \exp(J/T_N)$ for $y = 0$ (J is the in-plane exchange energy). When T_N is reduced to about 250 K by oxygen doping, a mesoscopic phase separation takes place so that $\xi(T_N) = L$ (see [67]), where L is the size of the antiferromagnetically correlated clusters, and depends only on the extra oxygen content y. In this case, we have $T_N = J'(L/a)^2$. Since L is independent of the isotope mass, a negligible isotope shift of T_N in the oxygen-doped La_2CuO_{4+y} suggests

that J' is independent of the isotope mass. Then we easily find for undoped compounds

$$\Delta T_N/T_N = (\Delta J/J)\frac{B}{1+B} \tag{6}$$

where $B = 2J/T_N \simeq 10$. From the measured isotope shift of T_N for the undoped samples, we obtain $\Delta J/J \simeq -0.6\%$.

Theoretically, Kugel and Khomski [68] considered the Jahn–Teller effect in a single-band Hubard model. They showed that, for $U \gg E_p, \hbar\omega$,

$$J = \frac{2t^2}{U}\left(1 + \frac{2E_p\hbar\omega}{U^2}\right). \tag{7}$$

On the other hand, when $U \ll \hbar\omega$,

$$J = \frac{2t^2\exp(-2E_p/\hbar\omega)}{U - 2E_p}. \tag{8}$$

Here U is the onsite Coulomb repulsion, t is the bare hopping integral, E_p is the Jahn–Teller stabilization energy and ω is the vibration frequency of the Jahn–Teller mode. Assuming $t = 0.5$ eV and $J = 0.13$ eV, we obtain $U = 3.8$ eV. With $\hbar\omega = 0.1$ eV and $E_p = 1.2$ eV [69], we obtain $\Delta J/J \simeq -0.1\%$ from equation (7), which is about a factor of six smaller than the measured value. The discrepancy might be due to the fact that the single-band Hubard model is oversimplified for the parent cuprates.

10. Concluding remarks

In summary, the unconventional isotope effects observed in cuprates clearly demonstrate that the electron–phonon interaction plays an important role in the physics of cuprates. Our results also show that the phonon modes related to both oxygen and copper vibrations are important to the pairing.

Interestingly, the concept of enhancing the electron–phonon coupling was the original motivation for the discovery of high-T_c. Bednorz and Müller [1] argued that there should be a strong electron–phonon interaction in perovskites with strong Jahn-Teller centres. Indeed, the stretching vibration mode, which is related to the Q_2-type Jahn–Teller distortion, has proved to couple strongly to the doped holes [70–72]. This high-energy Q_2-type mode may couple to the low-energy tilting mode (Q_4/Q_5-like Jahn–Teller mode) if the Cu–O–Cu bonding angle is less than 180°. Thus both stretching and tilting modes are important to high-T_c superconductivity.

Acknowledgments

The authors would like to thank K A Müller, A Shengelaya, J Hofer, A Bianconi and D E Morris for their collaborations and discussions. The work was supported by the Swiss National Science Foundation.

References

[1] Bednorz J G and Müller K A 1986 *Z. Phys.* B **64** 189
[2] Batlogg B *et al* 1987 *Phys. Rev. Lett.* **58** 2333
[3] Bourne L C *et al* 1987 *Phys. Rev. Lett.* **58** 2337
[4] Morris D E *et al* 1988 *Phys. Rev.* B **37** 5936
[5] Schrieffer J R, Wen X G and Zhang S C 1989 *Phys. Rev.* B **39** 11 663
[6] Millis A J, Monien H and Pines D 1990 *Phys. Rev.* B **42** 167

[7] Anderson P W 1998 *The Theory of Superconductivity in the High-T_c Cuprate Superconductors* (Princeton, NJ: Princeton University Press)
[8] Carbotte J P 1990 *Rev. Mod. Phys.* **62** 1027
[9] Daunt J G and Mendelssohn K 1946 *Proc. R. Soc.* A **185** 225
[10] Maxwell E 1950 *Phys. Rev.* **78** 477
[11] Reynolds C A, Serin B, Wright W H and Nesbitt L B 1950 *Phys. Rev.* **78** 487
[12] Fröhlich H 1950 *Phys. Rev.* **79** 845
[13] Cooper L N 1956 *Phys. Rev.* **104** 1189
[14] Schafroth M R 1955 *Phys. Rev.* **100** 463
[15] Bardeen J, Cooper L N and Schrieffer J R 1957 *Phys. Rev.* **108** 1175
[16] Alexandrov A S and Mott N F 1995 *Polarons and Bipolarons* (Singapore: World Scientific)
[17] Franck J P 1994 *Physical Properties of High Temperature Superconductors IV* ed D M Ginsberg (Singapore: World Scientific) p 189
[18] Müller K A 1990 *Z. Phys.* B **80** 193
[19] Zhao G M, Conder K, Angst M, Kazakov S M, Karpinski J, Maciejewski M, Bougerol C, Pshirkov J S and Antipov E V 2000 *Phys. Rev.* B **62** R11 977
[20] Crawford M K, Kunchur M N, Farneth W E, McCaron E M III and Poon S J 1990 *Phys. Rev.* B **41** 282
[21] Bornemann H J, Morris D E, Liu H B and Narwankar P K 1992 *Physica* C **191** 211
[22] Franck J P, Harker S and Brewer J H 1993 *Phys. Rev. Lett.* **71** 283
[23] Zech D, Conder K, Keller H, Kaldis E, Liarokapis E, Poulakis N and Müller K A 1995 *Proceedings Int. Workshop on Anharmonic Properties of High-T_c Cuprates* ed D Mihailović *et al* (Singapore: World Scientific) p 18
[24] Zech D, Conder K, Keller H, Kaldis E and Müller K A 1996 *Physica* B **219–220** 136
[25] Zhao G M, Singh K K, Sinha A P B and Morris D E 1995 *Phys. Rev.* B **52** 6840
[26] Zhao G M, Hunt M B, Keller H and Müller K A 1997 *Nature* **385** 236
[27] Zhao G M, Conder K, Keller H and Müller K A 1998 *J. Phys.: Condens. Matter* **10** 9055
[28] Pickett W E, Cohen R E and Krakauer H 1991 *Phys. Rev. Lett.* **67** 228
[29] Zhao G M, Kirtikar V, Singh K K, Sinha A P B, Morris D E and Inyushkin A V 1996 *Phys. Rev.* B **54** 14 956
[30] Morris D E, Sinha A P B, Kirtikar V, Singh K K and Inyushkin A V 1998 *Physica* C **298** 203
[31] Williams G V M, Pringle D J and Tallon J L 2000 *Phys. Rev.* B **61** R9257
[32] Cardona M, Liu R, Thomsen C, Kress W, Schönherr E, Bauer M, Genzel L and König W 1988 *Solid State Commun.* **67** 789
[33] Ham W K, Keller S W, Michaels J N, Stacey A M, Krillov D, Hodul D T and Fleming R H 1989 *J. Mater. Res.* **4** 504
[34] Nickel J H, Morris D E and Ager J W III 1993 *Phys. Rev. Lett.* **70** 81
[35] Zech D, Keller H, Conder K, Kaldis E, Liarokapis E, Poulakis N and Müller K A 1994 *Nature* **371** 681
[36] Zhao G M, Ager J W III and Morris D E 1996 *Phys. Rev.* B **54** 14 982
[37] Conder K, Rusiecki S and Kaldis E 1989 *Mater. Res. Bull.* **24** 581
[38] Zhao G M and Morris D E 1995 *Phys. Rev.* B **51** 16 487
[39] Shoenberg D 1940 *Proc. R. Soc.* A **175** 49
[40] Kogan V G, Fang M M and Mitra S 1988 *Phys. Rev.* B **38** 11 958
[41] Willemin M *et al* 1998 *J. Appl. Phys.* **83** 1163
[42] Hofer J, Conder K, Sasagawa T, Zhao G M, Willemin M, Keller H and Kishio K 2000 *Phys. Rev. Lett.* **84** 4192
[43] Zhao G M, Kirtikar V and Morris D E *Phys. Rev.* B **63** R220 506
[44] Tranquada J M, Sternlleb B J, Axe J D, Nakamura Y and Uchida S 1995 *Nature* **375** 561
[45] Mook H A, Dai P C, Hayden S M, Aeppli G, Perring T G and Dogan F 1998 *Nature* **395** 580
[46] Bianconi A, Saini N L, Lanzara A, Missori M, Rossetti T, Oyanagi H, Yamaguchi H, Oka K and Ito T 1996 *Phys. Rev. Lett.* **76** 3412
[47] Emery V J, Kivelson S A and Zachar O 1997 *Phys. Rev.* B **56** 6120
[48] Bussmann-Holder A, Simon A, Buttner H and Bishop A R 2000 *Phil. Mag.* B **80** 1955
Bussmann-Holder A, Müller K A, Micnas R, Buttner H, Simon A, Bishop A R and Egami T 2001 *J. Phys.: Condens. Matter* **13** L169
[49] Zhao G M, Ghosh K and Greene R L 1998 *J. Phys.: Condens. Matter* **10** L737
Zhao G M, Ghosh K, Keller H and Greene R L 1999 *Phys. Rev.* B **59** 81
[50] Lanzara A, Zhao G M, Saini N L, Bianconi A, Conder K, Keller H and Müller K A 1999 *J. Phys.: Condens. Matter* **11** L541
[51] Blawid S and Millis A J 2001 *Phys. Rev.* B **63** 115 114
[52] Temprano D R, Mesot J, Janssen S, Conder K, Furrer A, Mutka H and Müller K A 2000 *Phys. Rev. Lett.* **84** 1990
[53] Temprano D R, Mesot J, Janssen S, Conder K, Furrer A, Sokolov A, Trounov V, Kazakov S M, Karpinski J and

Müller K A 2001 *Eur. Phys. J.* B **19** 5
[54] Raffa F, Ohno T, Mali M, Roos J, Brinkmann D, Conder K and Eremin M 1998 *Phys. Rev. Lett.* **81** 5912
[55] Sichelschmidt J, Elschner B, Loidl A and Kochelaev Bl 1995 *Phys. Rev.* B **51** 9199
[56] Kochelaev B I *et al* 1997 *Phys. Rev. Lett.* **79** 4274
[57] Kochelaev B I *et al* 1994 *Phys. Rev.* B **49** 13 106
[58] Müller K A 2000 *Physica* C **341–348** 11
[59] Shengelaya A *et al* 2001 *Phys. Rev.* B **63** 144 513
[60] Sternlieb B J *et al* 1990 *Phys. Rev.* B **41** 8866
[61] Cho J H, Borsa F, Johnston D C and Torgeson D R 1992 *Phys. Rev.* B **46** 3179
[62] Zhao G M, Conder K, Keller H and Müller K A 1996 *Nature* **381** 676
[63] Shengelaya A, Zhao G M, Aegerter C M, Conder K, Savic I M and Keller H 1999 *Phys. Rev. Lett.* **83** 5142
[64] Zhao G M, Singh K K and Morris D E 1994 *Phys. Rev.* B **50** 4112
[65] Kramer S, Gyorfi K H, Bussmann-Holder A, Conder K and Mehring M 1999 *Phys. Status Solidi* b **215** 601
[66] Thio T *et al* 1988 *Phys. Rev.* B **38** 905
[67] Cho J H, Chou F C and Johnston D C 1993 *Phys. Rev. Lett.* **70** 222
[68] Kugel K I and Khomski D I 1980 *Sov. Phys.–JETP* **52** 501
[69] Kamimura H 1987 *Int. J. Mod. Phys.* B **1** 873
[70] Pintschovius L and Reichardt W 1994 *Physical Properties of High Temperature Superconductors IV* ed D Ginsberg (Singapore: World Scientific) p 295
[71] McQueeney R J, Petrov Y, Egami T, Yethiraj M, Shirane G and Endoh Y 1999 *Phys. Rev. Lett.* **82** 628
[72] Petrov Y, Egami T, McQueeney R J, Yethiraj M, Mook H A and Dogan F *Preprint* cond-mat/0003414